Scaffold hopping approach on the route to selective tankyrase inhibitors

12 AUTHORS, INCLUDING:

Paride Liscio
TES Pharma S.r.l.
8 PUBLICATIONS **29** CITATIONS

SEE PROFILE

Andrea Carotti
Università degli Studi di Perugia
45 PUBLICATIONS **487** CITATIONS

SEE PROFILE

Antonio Macchiarulo
Università degli Studi di Perugia
125 PUBLICATIONS **2,654** CITATIONS

SEE PROFILE

Roberto Pellicciari
Università degli Studi di Perugia
361 PUBLICATIONS **8,673** CITATIONS

SEE PROFILE

Original article

Scaffold hopping approach on the route to selective tankyrase inhibitors

Paride Liscio [a, d], Andrea Carotti [a], Stefania Asciutti [b], Martina Ferri [a], Maira M. Pires [b], Sara Valloscuro [b], Jacob Ziff [b], Neil R. Clark [c], Antonio Macchiarulo [a], Stuart A. Aaronson [b], Roberto Pellicciari [a, d], Emidio Camaioni [a, *]

[a] Department of Pharmaceutical Sciences, University of Perugia, Via del Liceo 1, 06123 Perugia, Italy
[b] Icahn School of Medicine at Mount Sinai, Department of Oncological Sciences, 1425 Madison Ave, New York, NY 10029, USA
[c] Icahn School of Medicine at Mount Sinai, Department of Pharmacology and Systems Therapeutics, 1425 Madison Ave, New York, NY 10029, USA
[d] TES Pharma, Via P. Togliatti 22bis, 06073 Terrioli, Corciano, Italy

ARTICLE INFO

ABSTRACT

A virtual screening procedure was applied to identify new tankyrase inhibitors. Through pharmacophore screening of a compounds collection from the SPECS database, the methoxy[l]benzothieno[2,3-c]quinolin-6(5H)-one scaffold was identified as nicotinamide mimetic able to inhibit tankyrase activity at low micromolar concentration. In order to improve potency and selectivity, tandem structure-based and scaffold hopping approaches were carried out over the new scaffold leading to the discovery of the 2-(phenyl)-3H-benzo[4,5]thieno[3,2-d]pyrimidin-4-one as powerful chemotype suitable for tankyrase inhibition. The best compound 2-(4-tert-butyl-phenyl)-3H-benzo[4,5]thieno[3,2-d]pyrimidin-4-one (23) displayed nanomolar potencies (IC$_{50s}$ TNKS-1 = 21 nM and TNKS-2 = 29 nM) and high selectivity when profiled against several other PARPs. Furthermore, a striking Wnt signaling, as well as cell growth inhibition, was observed assaying 23 in DLD-1 cancer cells.

© 2014 Elsevier Masson SAS. All rights reserved.

1. Introduction

Tankyrases (TNKS-1 and TNKS-2), also referred to as ADP-ribosyltransferases ARTD-5 and ARTD-6 respectively, are members of the poly (ADP-ribose)polymerases (PARPs) family [1,2]. By having an active role in telomere maintenance and Wnt pathway regulation, TNKSs take part in the complex arena of processes that orchestrate tissue differentiation and renewal [3]. Aberration of these processes may result in pathological settings such as those of many cancers. Therefore, inhibition of TNKSs activity has been recently proposed as a new promising strategy in the treatment of cancers [3]. Furthermore, the implication of TNKSs activity in a plethora of other conditions such as viral infection [4,5], tissue fibrosis [6] and glucose metabolism [7], make TNKSs attractive targets for therapeutic intervention. To this end, recent studies have allowed the identification of several classes of TNKSs

inhibitors with improved target selectivity and strong pharmacokinetic profile, although validation of TNKSs inhibition as a therapeutic strategy is still challenging. TNKSs inhibitors can be classified into three main groups: a) compounds that bind the well-known canonical PARP pharmacophore working as nicotinamide isosteres [8] such as lactam-based pyrimidin-4-one (XAV-939, 1) [9], 4-Methyl-7-phenyl-1H-quinolin-2-ones (2) [10], 2-phenyl-3,4-dihydroquinazolin-4-ones (3) [11] and non-lactam inhibitors such as [1,2,4]triazol-3-ylamines (4) [12] and triazolo[4,3-b]pyridazine amines (5) [13] (Fig. 1); b) compounds that bind to the adjacent induced pocket of the enzymes, including IWR-1/-2 [14–16], JW-74 [17], G007-LK [18] and 2-aminopyridine oxadiazolinones [19]; c) compounds that simultaneously occupy both sites aforementioned such as variously substituted 3-((4-oxo-3,4-dihydroquinazolin-2-yl)thio) propanamides derivatives, which are also known as dual binders, as previously exemplified [20]. Target specificity is a main issue in drug discovery, in particular in the field of PARP inhibitors, where the utilization of chemical tools with low selectivity between the PARP family members may give rise to off-target effects leading to erroneous data interpretation, raising polypharmacology questions [21]. Herein, as an extension of our work in the field [8,13] we applied a virtual screening
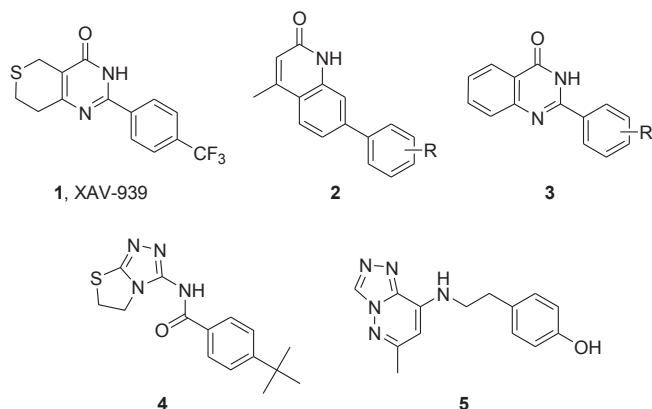
Fig. 1. Selected TNKS inhibitors that occupy the canonical nicotinamide binding pocket.

procedure with a minimal pharmacophore hypothesis to identify new chemical entities that inhibit TNKSs on the canonical nicotinamide binding pocket. Tandem structure based and scaffold hopping approaches have been applied in this study leading to the discovery of novel benzo[4,5]thieno[3,2-*d*]pyrimidin-4-ones as potent and selective tankyrase 1 and 2 inhibitors.

2. Results and discussion

2.1. Virtual screening

A virtual screening (VS) campaign was carried out using the crystal structures of TNKS-2 and TNKS-1 in complex with inhibitors acting only at the canonical and well characterized nicotinamide (NI) binding site of the protein. TNKS-1 and TNKS-2 co-crystal complexes with **1** [9] (PDB codes 3UH4 [22] and 3KR8 [23], respectively) were instrumental to start the generation of the pharmacophore model, using them as reference in the alignment phase of the protocol. A pharmacophore hypothesis was developed using the ligands extracted by 8 collected x-ray complexes after backbone superposition (PDB codes 3KR8 [23], 3UH4 [22], 3MHJ, 3MHK, 3P0N, 3P0P [8], 3U9H [14]). Selecting the points (shared by at least two inhibitors) the hypothesis was finally composed by a total of 8 interaction features, including 1 hydrogen bond donor (D3), 1 hydrogen bond acceptor (A2), 2 aromatic (R6 to R9) and 2 hydrophobic (H4 and H5) points (Fig. 2A). Excluded volumes were also added using the residues of the TNKS-2 binding site as detailed in the method section (Fig. 2B).

The minimum number of pharmacophore points to be matched by the virtual hits was set to 4, moreover two "must match" points

were set to the D3 and A2 points, the ones already observed to form hydrogen bonds with the Gly1032 (TNKS-2 numbering) of the TNKS enzyme (a common feature among most PARP inhibitors). Looking at the well known TNKS inhibitors, we frequently observed aromatic rings, or at least one aromatic ring and a hydrophobic group. Therefore at least two more other points were added to be match by the putative binders. Next, more than 210,000 of commercially available compounds were funneled through the pharmacophoric model, resulting in 29,973 compounds identified as virtual hits. These compounds were further submitted to a structure-based screening, consisting of a docking of the molecules into the TNKS-2 crystal structure (PDB code 3KR8 [23]). From the list of docking scores, 299 compounds were chosen having a higher ranking score with respect to the one obtained by the co-crystallized **1** with the TNKS-2 binding site. Among them, 34 compounds were selected and purchased on the basis of chemical diversity using a Tanimoto cut-off of 0.8. The activity of these compounds was then evaluated using TCF-luciferase reporter construct generated in our laboratory to assess Wnt activity. Six compounds were found to reduce TCF transcriptional activity (>20%) at a concentration of 10 μM and were then tested using a biochemical assay to ascertain their TNKSs inhibition potency at 1 μM. As a result, only the two benzo[*b*]thieno[2,3-*c*]quinolin-6(5*H*)-ones derivatives (**6** and **7**, Table 1) were able to inhibit the two TNKSs. These two compounds were also profiled *in vitro* on the main PARP isoforms as reported in Table 1.

Thus, compounds **6** and **7** displayed a marked inhibition of TNKS (>70% on both isoforms) endowed with an interesting selectivity profile toward the two main PARP enzymes (PARP-1 and -2). Once validated as novel scaffold for the inhibition of TNKS proteins, **6** and **7** were submitted to an optimization program mainly focused on the rational modification of the benzo[*b*]thienoquinolinone polycyclic core.

2.2. Hit optimization by structure-based and scaffold-hopping approaches

First round of exploration: with the main purpose of increasing the inhibitory potency while maintaining the selectivity profile *vs* TNKS isoforms of PARP, the corresponding hydroxyl derivatives of **6** and **7** were prepared (compounds **8** and **9**, respectively Table 2). To characterize the structural details of the TNKS specificity displayed by **6** and **7**, the two methoxy group were combined together in derivative **10** (Table 2) and completely removed in the unsubstituted benzo[*b*]thieno[2,3-*c*]quinolin-5(6*H*)-one (**11**) (Fig. 3 and Table 2) that was also selected as a reference compound for the structure activity relationship (SAR) profile.

Second round of exploration: with the aim of gaining insight into the role played by the benzo[*b*]thieno[2,3-*c*]quinolin-5(6*H*)-
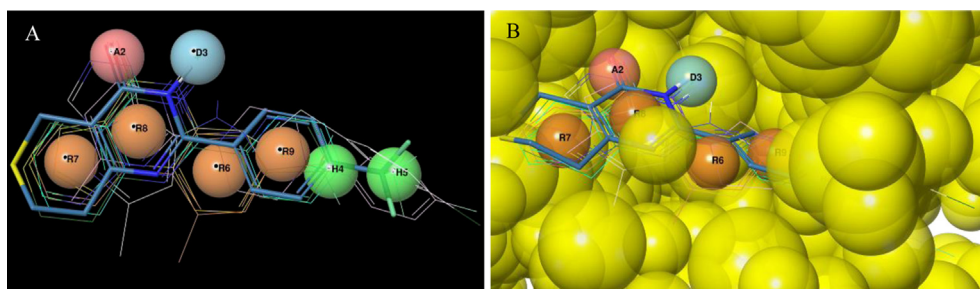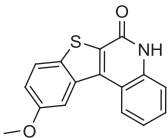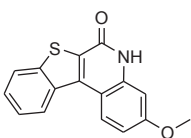

Fig. 2. (A, left panel) Pharmacophore hypothesis: 1 hydrogen bond acceptor (A2, red dot), 1 hydrogen bond donor (D3, cyan dot), 4 aromatic (R6–R9, orange dot), 2 hydrophobic (H4–H5, green dot). Ligands color legend: 3KR8 blue (sticks), 3UH4 cyan, 3MHJ orange, 3MHK green, 3P0N yellow, 3P0P pink, 3P0Q white, 3U9H green. (B, right panel) Excluded volumes (yellow dots) were generated by the superimposed crystal complexes, as detailed in the method section. (For interpretation of the references to color in this figure legend, the reader is referred to the web version of this article.)

Table 1
PARPs profiling of benzo[b]thieno[2,3-c]quinolin-6(5H)-ones based derivatives.

Compounds	% of inhibition[a]				% of TCF inhibition ± SD[b]	Log $D_{7.4}$
	PARP-1	PARP-2	TNKS-1	TNKS-2		
6	13	17	76	72	21 ± 6.3	3.59
7	16	27	92	83	37 ± 17.6	3.59

[a] Data are from experiments conducted in duplicate at concentration of 1 μM.
[b] Data are from DLD-1 colorectal cancer cells treated with each compound at 10 μM concentration for 24 h. Data reflect the average of at least three separate experiments combined.

one polycyclic ring system in driving TNSKs activity and selectivity, in the second task of this work, a scaffold hopping approach was applied and a new small library of six compounds (**12**–**17**) based on the thienopyridinone template was further designed and synthesized, according to Fig. 3.

According to this strategy, the polycyclic basic core of compound **11** has been simplified removing cycle by cycle (red, green, blue; Fig. 3) while keeping constant the minimal pharmacophoric requirement for TNKSs inhibition (aromatic amide moiety in *anti* conformation). Furthermore, inspired from the work by Lehtiö et al. [11] on 2-phenyl quinazolinones as TNKS inhibitors, an additional phenyl ring (black) has been introduced in position C-3 and C-5 of compound **14** and **15** respectively thus affording new chemical entities such as **16** and **17** (Fig. 3). Next, a nitrogen atom has been also introduced in position C-4 of **16** leading to the corresponding benzo[4,5]thieno[3,2-d]pyrimidin-4-one nucleus where **18** (Table 3) is the parent compound. Then **18** has been advanced to a traditional process of structure-activity optimization in order to build a minimal SAR profile. Disruption of molecular planarity or symmetry may be taken into account as a valuable strategy for the pursuit of more soluble compounds. Thus, 2-phenyl-6,7,8,9-tetrahydro-3H-benzo[4,5]thieno[3,2-d]pyrimidin-4-one **19** and 2-cyclohexyl-3H-benzo[4,5]thieno[3,2-d]pyrimidin-4-one **20** were prepared from this reasoning (Table 3). Subsequently, bioisosteric replacement of the phenyl ring in C-2 position of compound **18** with a thiophene nucleus afforded compound **21** (Table 3). Finally, from the exhaustive examination of the structural data available on TNKS-inhibitor complexes, a methyl and *tert*-butyl [11] group have been selected as the optimal substituents for the *para*-position of the distal phenyl ring of compound **18** leading to the synthesis of the corresponding analogs **22** and **23** (Table 3).

2.3. Chemistry

All benzo[b]thieno[2,3-c]quinolin-5(6H)-one derivatives (**6**–**7**, **10**–**11**) were acquired or prepared according to previously published protocols [24–26] (Scheme 1 and Scheme S1 of supporting information, SI). The hydroxyl derivatives **8** and **9** were prepared in moderate yields, as reported in Scheme 1. Commercially available cinnamic acids **24** and **25** were oxidized by the action of thionyl chloride to afford the corresponding 3-chloro-benzo[b]thiophene-2-carbonyl chlorides **26** and **27**, in moderate yields [26]. Carboxamide derivatives **28** and **29** were easily prepared in high yield by refluxing **26** and **27** in benzene with the suitable anilines. Photochemical dehydrohalogen reaction [26] of the latter intermediates

furnished the methoxy benzo[b]thieno[2,3-c]quinolin-5(6H)-ones **6** and **7** which upon boron tribromide treatment gave the desired hydroxyl compounds **8** and **9**.

According to our purpose, thieno[2,3-c]quinolin-4(5H)-one (**12**, Fig. 3) [27], 4-phenylquinolin-2(1H)-one (**13**, Fig. 3) [28], 6H-thieno[2,3-c]pyridin-7-one (**15**, Fig. 3) [29] and 5-phenyl-6H-thieno[2,3-c]pyridin-7-one (**17**, Fig. 3) [30] were synthesized as reported in literature (Schemes S2–S5 of SI).

2H-benzo[4,5]thieno[2,3-c]pyridin-1-one (**14**) was prepared according to the synthetic procedure depicted in Scheme 2. Knoevenagel reaction between benzo[b]thiophene-3-carbaldehyde (**30**) and malonic acid was accomplished in the presence of catalytic amount of piperidine by using pyridine as solvent. The obtained *trans* acrylic acid intermediate **31** was then submitted to the acyl azide formation followed by an intramolecular cyclization *via* Curtius rearrangement to furnish the final compounds **14** in acceptable yields.

The synthesis of 3-phenyl-2H-benzo[4,5]thieno[2,3-c]pyridine-1-one (**16**) was performed according to the procedure depicted in Scheme 3. Intermolecular cyclization of 3-methylbenzo[b]thiophene-2-carboxylic acid (**32**) with benzonitrile (**33**) occurred in THF using 2 equivalent of *n*-buthyllithium and a catalytic amount of diisopropylamine thus providing the pyridinone **16**, in moderate yield.

The synthesis of 2-substituted-3H-benzo[4,5]thieno[3,2-d]pyrimidin-4-one based derivatives **18** [31], **20**-**23** was carried as depicted in Scheme 4.
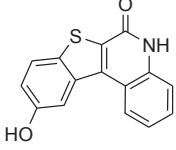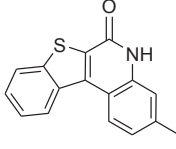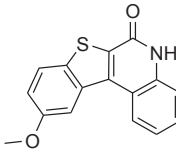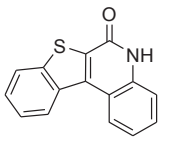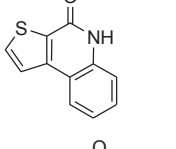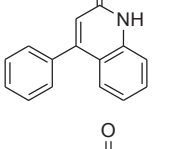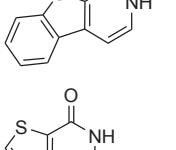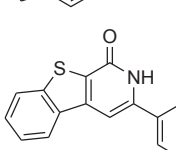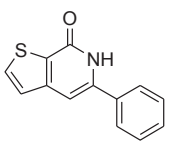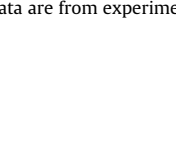
Reaction of 2-fluorobenzonitrile (**34**) with methylthioglycolate (**35**) afforded in high yield the key intermediate **36**. Amide bond formation was affected by the reaction of methyl-3-amino carboxybenzo[b]thiophene (**36**) and suitable carbonyl chlorides. The so formed carboxy amides **37**-**41** were submitted to intramolecular cyclization upon treatment with methanolic ammonia solution, furnishing the corresponding derivatives **18**, **20**–**23** (Table 3) in acceptable yields.

The synthesis of 2-phenyl-6,7,8,9-tetrahydro-3H-benzo[4,5]thieno[3,2-d]pyrimidin-4-one (**19**) was achieved, as reported in Scheme 5.

44 was easily prepared in two steps, starting from cyclohexanone (**42**) according to a literature protocol [32]. Reacting **44** with methylthioglycolate gave the 3-amino-4,5,6,7-tetrahydro-benzo[b]thiophene-2-carboxylic acid methyl ester (**45**), in almost quantitative yield. As previously reported, amide bond formation, and subsequent intramolecular cyclization furnished the desired derivative **19**.

Table 2
Inhibition data of synthesized derivatives at 1 μM concentration against recombinant human TNKS-1/-2, and PARP-1/-2.

Compounds	% of inhibition[a]				Log $D_{7.4}$
	PARP-1	PARP-2	TNKS-1	TNKS-2	
8	95	93	89	91	3.44
9	52	64	100	91	3.43
10	12	12	83	64	3.43
11	7	14	100	92	3.75
12	75	91	79	83	2.65
13	3	3	0	1	3.03
14	26	34	29	27	3.62
15	11	24	14	19	1.24
16	3	11	84	79	3.63
17	12	26	33	50	2.53

[a] Data are from experiments conducted in duplicate at concentration of 1 μM.
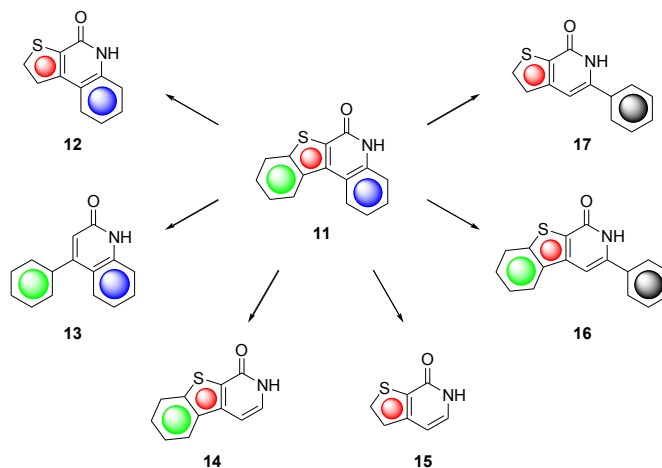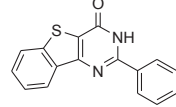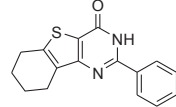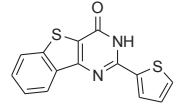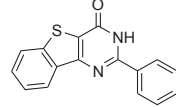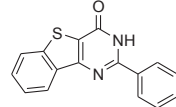
Fig. 3. Scaffold hopping approach for benzo[*b*]thieno[2,3-c]quinolin-5(6*H*)-one simplification.

2.4. Pharmacology

All newly synthesized compounds **8**–**23** were preliminary screened *in vitro* at the low concentration of 1 μM against TNKS-1/2 and PARP-1/2 enzymes with the purpose of a lead compound discovery. **1** was used in the assay as reference compound for the two TNKSs (100% of enzyme inhibition at 1 μM), and AZD 2281 (**24**,

Table 3
Inhibition data of thieno[3,2-*d*]pyrimidin-4-one derivatives at 1 μM concentration against recombinant human TNKS-1/-2 and PARP-1/-2.

Compounds	% of inhibition[a]				Log $D_{7.4}$
	PARP-1	PARP-2	TNKS-1	TNKS-2	
18	3	0	79	47	3.62
19	13	11	13	12	4.11
20	13	14	6	15	3.89
21	11	9	86	66	3.52
22	4	4	98	81	4.13
23	0	4	98	88	5.16

[a] Data are from experiments conducted in duplicate at concentration of 1 μM.

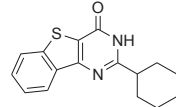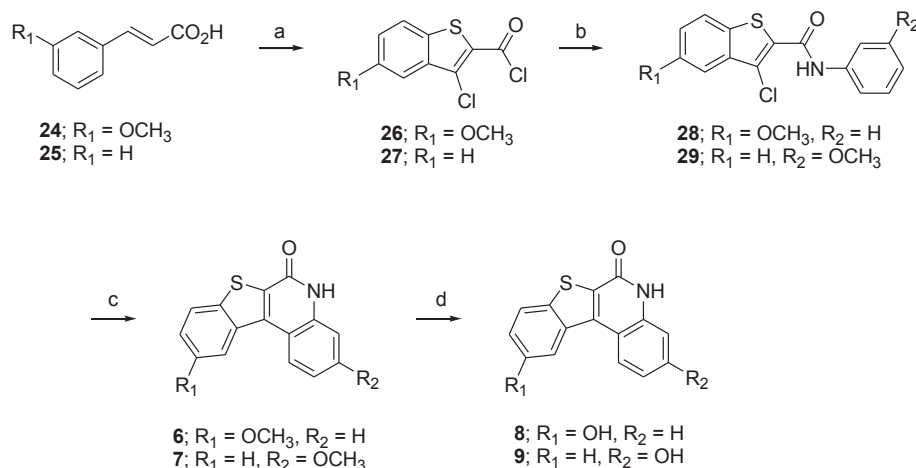**Scheme 1.** Synthesis of substituted benzo[*b*]thieno[2,3-*c*]quinolin-6(5*H*)-one derivatives. Reagents and conditions: a) SOCl₂, Py, 16 h − 3 days, reflux; b) m-anisidine or aniline, benzene, 2−8 h, reflux; c) hν, (450 W), acetone, 5 h; d) BBr₃, CH₂Cl₂, 16 h, rt.

Olaparib, chemical structure on Fig. 2S of SI) [33] for PARP-1 and -2 (100% of inhibition at 20 nM on both PARP-1 and -2). Inhibition data of the new compounds are reported in Tables 2 and 3.

With the aim of improving the starting physicochemical properties of **6** and **7** (Table 1) the more polar hydroxyl analogs were prepared (derivatives **8** and **9**, Table 2). However, despite the improvement in both potency (up to 90 and 100% of inhibition of TNKS-1 for **8** and **9**, respectively) and solubility (as shown by the lowering of the LogD values), the introduction of hydrophilic substituents abrogated any form of selectivity, according to the literature of well characterized PARP and TNKS inhibitors [8]. The introduction of two methoxy groups in position C-3 and C-10, respectively on the benzo[*b*]thieno[2,3-*c*]quinolin-5(6*H*)-one core (derivative **10**, Table 2) maintained the starting selectivity profile of **6** and **7** (Table 2). The same trend was also observed by the unsubstituted analog **11**, which stands out as the most potent compound of this series, showing at 1 μM, full inhibition of TNKS-1 and 91% inhibition of TNKS-2, while resulting nearly inactive on PARP-1/2.

Moving next to address the importance of the benzo[*b*]thieno [2,3-*c*]quinolin-5(6*H*)-one scaffold in driving isoform selectivity, we undertook a brief examination of the tetracyclic ring system by using a scaffold hopping approach, as exemplified by derivatives **12**-**17** (Fig. 3, Table 3). Removal of the left side hand phenyl ring of **11**, derivative **12** (Table 2), while preserving acceptable values of inhibitory percentage (ranging from 79 to 83% of inhibition at TNKS-1 and -2, respectively) abolished also any form of selectivity toward PARP-1 and -2 as recently supported for the quite similar structure of pan-PARP inhibitor phenanthridinone (PDB code 4AVU) [34]. On the contrary, removal of the right hand phenyl ring of the quinoline moiety, as in compound **14** (Table 2), decreased both selectivity and inhibitory activity. Low molecular weight

derivatives, such as **15** and **17**, suffered from poor potency and enzyme specificity, providing large support of literature data produced on this regard [8]. Depletion of the condensed thienyl ring from the starting compound **11**, allowed us to obtain the corresponding simplified 4-phenyl-1*H*-quinolin-2-one analog **13**. Despite it possessed all chemical features necessary to the binding in catalytic domain of PARPs, no activity was recorded, pointing out the key role played by the fused thiophene ring.

Starting from **11**, a scaffold hopping approach enabled us to identify a benzo[*b*]thieno[2,3-*c*]pyridin-1-one derivative (**16**, Table 2) as a novel scaffold suitable for TNKS inhibition. Considering the well documented DNA binding and topoisomerase poisoning properties of polycyclic like compounds (such as **10** and **11**) [35], compound **16** with high percentages of TNKS inhibition (84% of inhibition at TNKS-1 and 79% inhibition at TNKS-2, respectively) with respect to the PARP ones, was submitted to further chemical modifications with the goal of selecting a new lead compound for cellular assays. Therefore, six new analogs, **18**-**23**, were synthesized and screened as previously described at 1 μM concentration and the results are reported in Table 3.

Passing from the thieno[2,3-*c*]pyridin-1-one scaffold of **16** (Table 2) to the thieno[3,2-*d*]pyrimidin-4-one core of compound **18** (Table 3), we did not observe changes in the inhibitory percentages and selectivity while little improvement of the drug likeness was recorded. The disruption of molecular planarity adopted as a strategy to pursue more soluble compounds such as **19** and **20** (Table 3), led to nearly inactive compounds. From previous published data on TNKSs inhibition [11] we envisioned that the C-4 position of the distal phenyl ring would tolerate hydrophobic substituents such as a methyl or *tert*-butyl groups, as shown by derivatives **22** and **23** (Table 3). Accordingly, an improvement of the inhibitory percentages to TNKS inhibition was recorded for both compounds, while preserving the starting selectivity profile toward
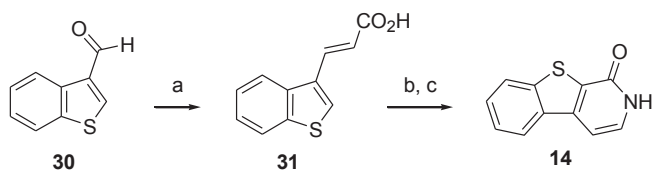
Scheme 2. Synthesis of 2*H*-benzo[4,5]thieno[2,3-*c*]pyridin-1-one (**14**). Reagents and conditions: a) Malonic acid, piperidine, py, 15 min, 0 °C, then 2 h, reflux; b) Et₃N, EtOCOCl, acetone, 20 min, rt, NaN₃, 30 min, 0 °C to rt; c) *n*Bu₃N, Ph₂O, 30 min, 230 °C.
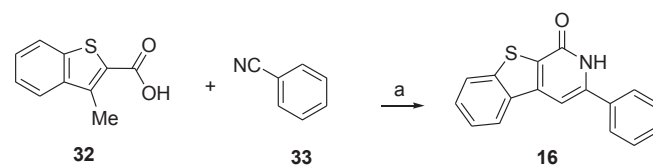
Scheme 3. Synthesis of 3-phenyl-2*H*-benzo[4,5]thieno[2,3-*c*]pyridine-1-one (**16**). Reagents and conditions: a) *n*-BuLi, DIPA, THF, 24 h, from 0 to −78 °C then rt.
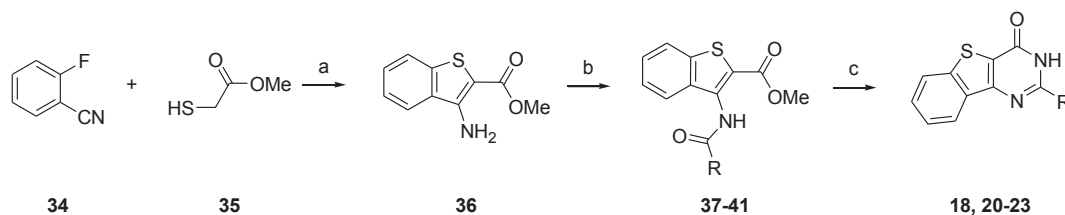
Scheme 4. Synthesis of 2-substituted-3*H*-benzo[4,5]thieno[3,2-*d*]pyrimidin-4-one derivatives (**18**, **20**–**23**). Reagents conditions: a) KOH, DMF, 1 h, 0 °C; b) RCOCl, Et₃N, CH₂Cl₂, 24–48 h; c) 30% NH₄OH, MeOH, 16 h, reflux.
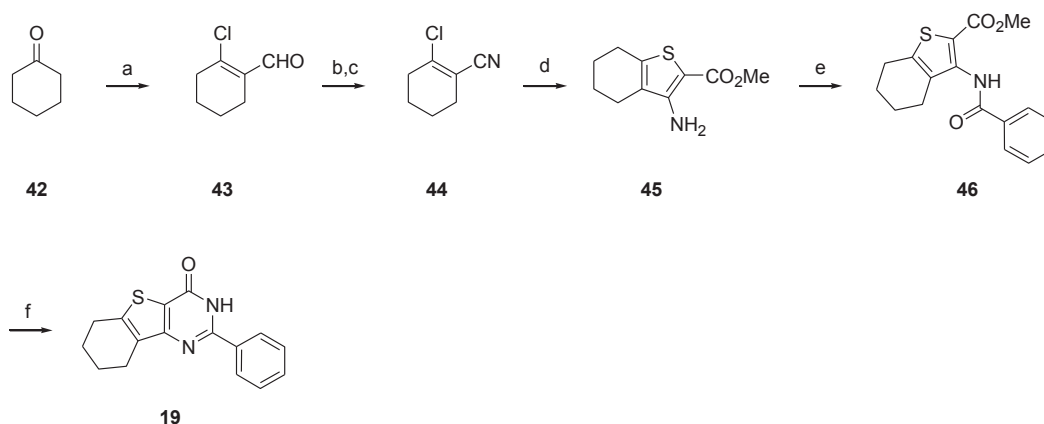
Scheme 5. Synthesis of 2-phenyl-6,7,8,9-tetrahydro-3*H*-benzo[4,5]thieno[3,2-*d*]pyrimidin-4-one (**19**). Reagents and conditions: a) DMF, POCl₃, 0 °C then 40 min rt; b) NMP, NH₂OH·HCl, 8 h, 115 °C. c) Ac₂O, 20 h, reflux; d) SHCH₂COOMe, K₂CO₃, MeOH, THF, 16 h, reflux; e) PhCOCl, Et₃N, DCM, 48 h; f) 30% NH₄OH, MeOH, 16 h, reflux.

PARP-1/2 enzymes. Among all synthesized derivatives, the most representative compound of each series (derivatives **11**, **16**, **22** and **23**) was selected for further biological characterizations. At first, full dose–response curves against TNKS-1 and -2 were determined for each one resulting in low nanomolar values of IC$_{50s}$ at TNKS enzymes (ranging from 20 to 200 nM, Table 4). Among them, 2-(4-*tert*-butyl-phenyl)-3*H*-benzo[4,5]thieno[3,2-*d*]pyrimidin-4-one (**23**) with IC$_{50}$ values of 21.3 and 28.6 nM on TNKS-1 and -2, respectively (Table 4 and Fig. 1S of SI) resulted to be the most effective TNKS inhibitor of the series. **23** also showed an improved profile of selectivity with respect to compound **1** *versus* PARP-1 and -2, and thus it was chosen for further biological studies.

Successively, the selectivity of **23** was further evaluated against a panel of additional PARP enzymes (1-3, 6-8, 10-12, 14; Fig. 4). Interestingly, TNKS proteins were already fully inhibited at the concentration of 10 μM by compound **23** whereas at higher concentrations it displayed only a minimal inhibition effect on the other PARPs tested (below 20% at 10 μM).

Taking into account these findings, we further investigated compound **23** by measuring Wnt activity using a TCF-reporter luciferase assay. Previous seminal works [9,14] showed that Axin

stabilization by TNKS inhibitors can antagonize canonical Wnt signaling to reduce proliferation of Wnt-activated DLD-1 cancer cells. To evaluate the effect of our most potent compound **23** on TCF-dependent transcriptional activity, DLD-1 colorectal cancer cells were incubated with increasing dose of compound **23** for 24 h (Fig. 5A). IC$_{50}$ values of the three compounds have been determined revealing comparable activities (Fig. 5A). However in our hands limited Wnt inhibition was detected at concentrations lower than 1 μM (Fig. 5A), while exactly at 1 μM the new compound **23** inhibited TCF reporter activity in a comparable fashion to the reference compounds **1** and IWR-1 (**25**, chemical structure on Fig 2S of SI). To further investigate the effects of our compound in long-term growth inhibition experiments, DLD-1 cancer cells were subjected to increasing concentrations of 1, 5, and 10 μM of compound **23**. A marked efficacy was observed for compound **23** as shown in Fig. 5B. The Wnt-negative RKO colorectal cancer cell line was used as negative control and marginal non-specific effects were only detected at concentrations higher than 10 μM (Fig. 5C).

Furthermore, to gain insights about the binding site disposition of compound **23**, we performed a docking study using the TNKS-2/XAV939 crystal structure (PDB code 3KR8 [21]), with the same settings applied during the virtual screening workflow (Fig. 6). Notably, the top ranked pose orients its *tert*-butyl moiety into a hydrophobic region defined by the Ile1075, Phe1035 and Tyr1051 together with the bidentate hydrogen bond interaction with the Gly1032, as already observed in other PARP inhibitors. Two π–π stacking interactions are taking place between the Tyr1071 and the pyrimidin-4-one ring, and the Tyr1060 with the 3*H*-benzo[4,5] thieno core of the molecule. The *tert*-butyl moiety orientation was also highlighted by Haikarainen et al. in a published TNKS-2 crystal complex (PDB code 4BUD) [11] (Fig. 6). All these interactions are essential to gain the potency and the selectivity of this series of compounds, however further investigations are needed to fully understand the molecular determinants of the observed profiles.

Table 4
Comparative inhibition data of compounds **11**, **16**, **22**, **23** and XAV939 (**1**) against PARP-1/2 and TNKS-1/2.

Compd	PARP-1	PARP-2	TNKS-1	TNKS-2
	% of inhibition[a]		(IC$_{50}$, nM)	(IC$_{50}$, nM)
11	–	–	90	180
16	–	–	181	283
22	–	–	19.4	79.8
23	0	0	21.3	28.6
1	91	100	11.1	3.6

[a] Data are from experiments conducted in duplicate at concentration of 10 μM.
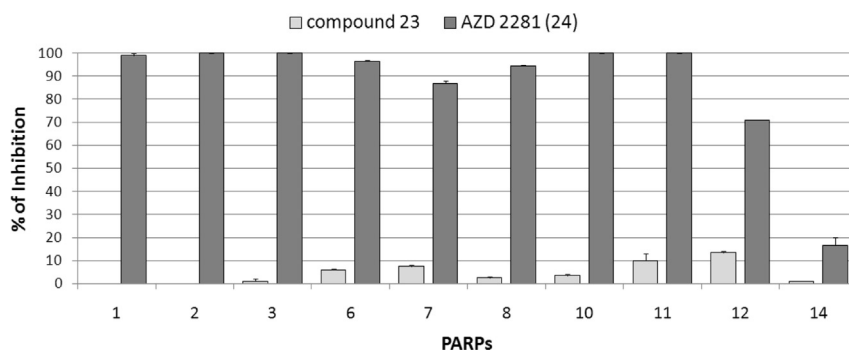
Fig. 4. PARP selectivity profile of compound **23**. Compound **23** was tested in duplicate at 10 μM concentration against several members of the PARP superfamily; AZD 2281 (**24**) was used as positive control and it was tested at a concentration about 10 times higher than its relative IC_{50s} on the corresponding PARP (1–3, 6–8, 10–12), with exception of PARP-14 where compound **24** inhibited less than 20% at 100 μM (further details on Table 2S of SI).

3. Conclusion

Herein we have reported the identification of 2-phenyl-3*H*-benzo[4,5]thieno[3,2-*d*]pyrimidin-4-ones as a novel class of selective TNKS-1/2 inhibitors. A sequential focused virtual screening approach with a minimal binding pharmacophore hypothesis on the canonical nicotinamide pocket of TNKSs led us to the identification of two [*l*]benzothieno[2,3-*c*]quinolin-6(5*H*)-one based hit compounds **6** and **7** as potent and selective TNKS inhibitors. Starting from these data, an explorative project has been made up on route to a potential lead compound discovery. Tandem structure-based and scaffold hopping approaches have been applied, thus enabling the discovery of 2-(4-*tert*-butylphenyl)-3*H*-benzo[4,5]thieno[3,2-*d*]pyrimidin-4-one (**23**) as a novel TNKS inhibitor. Compound **23** demonstrated excellent TNKS potency in an enzymatic assay (with IC_{50} in the nanomolar range of potency) and a clean profile of activity within the PARP superfamily, resulting in Wnt signaling inhibition and cell growth inhibition in DLD-1 colon cancer line. All these findings support compound **23** as a powerful chemical tool in investigating the role of TNKS in pathological settings. Furthermore the 2-(phenyl)-3*H*-benzo[4,5]thieno[3,2-*d*]pyrimidin-4-one could be suggested as a new privileged nucleus for tankyrase inhibition worthy for further medicinal chemistry program.

4. Experimental protocols

4.1. Chemistry

^{1}H NMR spectra were recorded at 200 and 400 MHz and ^{13}C NMR spectra were recorded at 100.6 and 50.3 MHz using the solvents

TOP (LUC/RL) IC_{50} (μM ± SD)	
XAV-939 (**1**)	0.707 ± 0.048
IWR-1 (**25**)	0.685 ± 0.047
23	0.832 ± 0.017
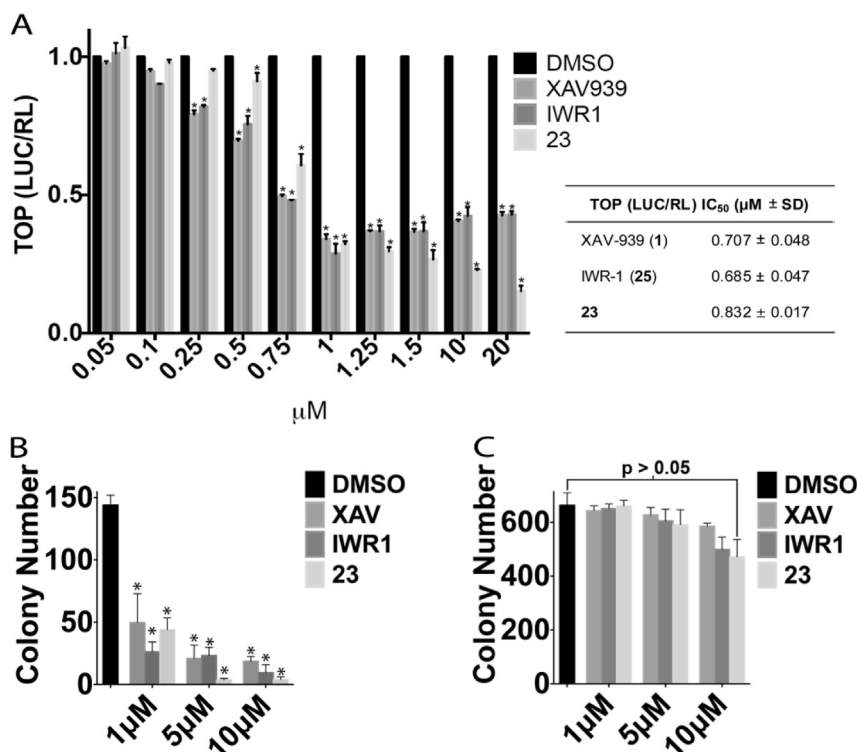
Fig. 5. (A) TOP/RL TCF-luciferase analysis showing significant reduction of Wnt activity after 24 h of treatment; $p < 0.05$. (B) Cell growth inhibition of DLD-1 colon tumor cells. (C) Cell growth inhibition of Wnt-negative RKO colorectal cancer cell line by compound **23**. Compound **23** was compared with standard inhibitors (compounds **1** [9] and IWR-1 **25** [14]) in Wnt-activated DLD-1 cells and in Wnt-negative RKO cells. (DMSO was used as negative control and same volume, 1 μL, was used across all samples). Data for (A), (B) and (C) are expressed as mean ± SEM from at least three independent experiments.
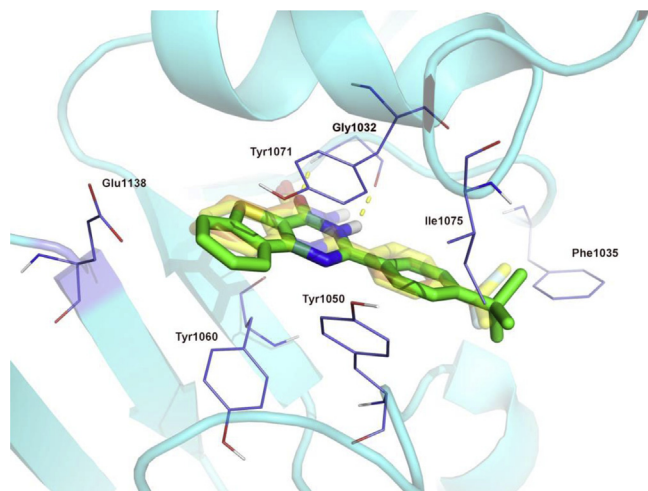
Fig. 6. Putative binding pose of compound **23** (green) inside the TNKS-2/XAV939 catalytic site. XAV939 (**1**) (orange) and para-*tert*-butyl-2-phenyl-3,4-dihydroquinazolin-4-one (yellow, PDB code 4BUD) inhibitors are also shown in transparent sticks. Key residues are shown in dark blue lines and labeled. Hydrogen bonds interactions are displayed by yellow dashes. (For interpretation of the references to color in this figure legend, the reader is referred to the web version of this article.)

indicated below. TLC were performed on aluminum backed silica plates (silica gel 60 F254). All the reaction were performed under nitrogen atmosphere using distilled solvent. All reagents were from commercial sources. All tested compounds were found to have >95% purity determined by HRMS (HPLC/Q-TOF) analyses. The LC system was an Agilent 1290 Infinity module equipped with an autosampler, a binary pump, a thermostated column compartment and a diode-array detector. The analytical column was a Zorbax Eclipse Plus (2.1 × 50 mm, 1.8 μm). The column temperature was maintained at 40 °C. The mobile phase consisted of an eluant A (water containing 0.1% formic acid) and an eluant B (acetonitrile plus 0.1% formic acid). A 0 min ($B = 20\%$) started a linear gradient at B 80% within 4 min, this mobile phase was maintained for 1 min, at the end of run (5 min) returned back to 20% B. The flow rate was of 0.25 mL/min. The LC system was connected to a detector Agilent 6540 UHD Accurate-Mass Q-TOF/MS system equipped with a source dual Jet Stream. The mass spectrometer operated with positive acquisition, Gas Temp 300 °C, gas flow 6.6 L/min, nebulizer pressure 16 psi, sheat gas temp 290 °C, fragmentor 200 V, Skimmer 65 V, Octapole RFPeaks 750, Capillary voltage 4000 V and Nozzle 0V and Reference masses 121.05087 and 922.009798. The analyses were performed by Mass Hunter workstation. The method EVAL (software Enhanced Chem-Station) was used to generate the gradient temperature in the GC−MS analysis on 6850/5975B apparatus (Agilent Technologies, Santa Clara, CA, USA).

4.2. 3-Chloro-5-methoxybenzo[b]thiophene-2-carbonyl chloride (26)

Thionyl chloride (13 mL, 179.2 mmol) was added, at room temperature, to a stirred mixture of 3-methoxycinnamic acid (**24**) (4 g, 22.4 mmol) and pyridine (0.36 mL, 4.5 mmol). After the addition was complete, the light yellow solution was heated between 100 and 102 °C for 16 h. The excess of thionyl chloride was removed under reduced pressure to give an orange solid. The solid was suspended in hot hexane, allowed to cool and stand at room temperature for 12 h. The yellow precipitate was collected by filtration. The title compound **26** was obtained in 87% yield (5.36 g, 19.49 mmol) used then without further purification. Analytical data are in agreement with those reported elsewhere [24,26].

4.3. 3-Chloro-benzo[b]thiophene-2-carboxylic acid methyl ester (27)

A stirred mixture of cinnamic acid (**25**) (6 g, 40.5 mmol), pyridine (0.32 ml, 4.05 mmol), thionyl chloride (11.6 mL, 96 mmol) in toluene (24 mL), was stirred at reflux for 3 days. The solvent was removed under reduced pressure. The mixture was suspended in hot Et₂O, and filtered. The title compound **27** was obtained in 47% yield (5 g, 19 mmol) as white solid, used then without further purification. Analytical data are in agreement with those reported elsewhere [24].

4.4. Preparation of substituted 3-chloro-N-phenylbenzo[b] thiophene-2-carboxamides 28 and 29

General procedure A: A solution of pyridine (11.5 mmol) in benzene (10 mL), was added dropwise to a stirred solution of the corresponding 3-chlorobenzo[b]thiophene-2-carbonyl chloride **26** or **27** (5.7 mmol) and m-anisidine or aniline (5.7 mmol) in the same solvent (50 mL). After the addition was complete, the mixture was heated at reflux from 2 to 8 h then allowed to cool to room temperature. The title compounds were obtained from moderate to good yields after filtration of the reaction mixture.

4.4.1. 3-Chloro-5-methoxy-N-phenylbenzo[b]thiophene-2-carboxamide (28)

Yield 88%; white solid. Analytical data are in agreement with those reported elsewhere [26].

4.4.2. 3-Chloro -N-(3-methoxyphenyl)benzo[b]thiophene-2-carboxamide (29)

Yield 48%; white solid. Analytical data are in agreement with those reported elsewhere [26].

4.5. Preparation of benzothieno[2,3-c]quinolin-6(5H)-ones 6 and 7

General procedure B: A stirred solution of the corresponding carboxamide **28** or **29** (1 mmol) and triethylamine (1 mmol) in acetone (500 mL) was irradiated under a slow stream of air for 5 h with a 450 W Hanovia medium pressure mercury vapor lamp. The precipitate was collected by filtration, washed with water (10 mL), then acetone (10 mL) and dried to give the corresponding compounds **6** and **7**, from moderate to good yields.

4.5.1. 10-Methoxy[l]benzothieno[2,3-c]quinolin-6(5H)-one (6)

Yield 64%; white solid, mp > 280 °C; ¹H NMR (400 MHz, DMSO-d_6) δ (ppm): 3.97 (s, 3H), 7.31 (d, $J = 7.5$ Hz, 1H), 7.39 (s, 1H), 7.54 (s, 2H), 8.11 (d, $J = 7.9$ Hz, 1H), 8.15 (s, 1H), 8.65 (d, $J = 6.7$ Hz, 1H), 12.2 (s, 1H); ¹³C NMR (100 MHz, DMSO-d_6) δ (ppm): 56.1, 108.5, 117.1, 117.5, 117.8, 123.1, 123.8, 125.2, 129.1, 133.8, 134.0, 135.9, 136.9, 137.9, 158.3, 158.3; MS (ESI⁺) m/z for C₁₆H₁₂NO₂S (M+H)⁺ calcd: 282.0583, found: 282.05806. Further analytical data are in agreement with those reported elsewhere [26].

4.5.2. 3-Methoxy[l]benzothieno[2,3-c]quinolin-6(5H)-one (7)

Yield 52%; white solid, mp > 280 °C; ¹H NMR (400 MHz, DMSO-d_6) δ (ppm): 3.86 (s, 3H), 6.99 (dd, $J_d = 2.5$ Hz, $J_d = 8.9$ Hz, 1H), 7.08 (d, $J = 2.5$ Hz, 1H), 7.66 (d, $J = 9.7$ Hz, 1H), 7.66 (m, 1H) 8.22 (dd, $J_d = 3.0$ Hz, $J_d = 7.1$ Hz, 1H), 8.67 (d, $J = 9$ Hz, 1H), 8.85 (dd, $J_d = 2.0$ Hz, $J_d = 5.8$ Hz, 1H), 12.1 (s, 1H); ¹³C NMR (100 MHz, DMSO-d_6) δ (ppm): 55.7, 100.3, 111.3, 111.9, 124.5, 125.4, 126.1, 126.2, 127.8, 129.7, 135.7, 136.6, 139.9, 141.8, 158.6, 159.9; MS (ESI⁺) m/z for C₁₆H₁₂NO₂S (M+H)⁺ calcd: 282.0583, found: 282.0598. Further analytical data are in agreement with those reported elsewhere [26].

4.6. Preparation of hydroxy[l]benzothieno[2,3-c]quinolin-6(5H)-ones **8** and **9**

General procedure C: BBr$_3$ (2 mmol) was added dropwise, at 0 °C, to a suspension of the corresponding methoxy[l]benzothieno [2,3-c]quinolin-6(5H)-one **6** or **7** in DCM as solvent. Stirring was continued for 16 h at room temperature. The excess of BBr$_3$ was carefully destroyed by the addiction of MeOH and a saturated solution of NaHCO$_3$. The solvent was removed under reduced pressure, the crude was suspended in water (100 mL) and extracted with EtOAc (3 × 20 mL). The organic layers were washed with brine, dried over Na$_2$SO$_4$ and concentrated under vacuum. The mixture was then purified by flash chromatography, eluting with DCM/MeOH, from 0 to 3%. The title compounds were obtained in moderate yields.

4.6.1. 10-Hydroxy[l]benzothieno[2,3-c]quinolin-6(5H)-one (**8**)
Yield 55%; white solid, mp > 280 °C; ^{1}H NMR (400 MHz, DMSO-d_6) δ (ppm): 7.19 (d, J = 8.7 Hz, 1H), 7.42 (t, J = 5.8 Hz, 1H), 7.56 (s, 2H), 8.01 (d, J = 8.7 Hz, 1H), 8.2 (s, 1H), 8.56 (d, J = 8.0 Hz, 1H), 9.85 (s, 1H), 12.17 (s, 1H); ^{13}C NMR (100 MHz, DMSO-d_6) δ (ppm): 111.1, 117.6, 118.4, 118.6, 123.5, 123.8, 125.6, 129.5, 130.5, 132.8, 136.1, 137.6, 138.4, 156.9, 158.8; MS (ESI$^+$) m/z for C$_{15}$H$_{10}$NO$_2$S (M+H)$^+$ calcd: 268,0424, found: 268,0351.

4.6.2. 3-Hydroxy[l]benzothieno[2,3-c]quinolin-6(5H)-one (**9**)
Yield 50%, white solid, mp > 280 °C; ^{1}H NMR (400 MHz, DMSO-d_6) δ (ppm): 6.87 (d, J = 8.9 Hz, 1H), 6.9 (s, 1H), 7.64 (m, 2H), 8.22 (m, 1H), 8.58 (d, J = 8.2 Hz, 1H), 8.84 (d, J = 5.0 Hz, 1H), 10.1 (s, 1H), 12.03 (s, 1H); ^{13}C NMR (100 MHz, DMSO-d_6) δ (ppm): 102.0, 110.9, 112.4, 124.5, 125.4, 126.0, 126.1, 127.7, 128.9, 135.8, 136.9, 140.0, 141.8, 158.5, 158.7; MS (ESI$^+$) m/z for C$_{15}$H$_{10}$NO$_2$S (M+H)$^+$ calcd: 268.0427, found: 268.0426.

4.7. 3-Benzo[b]thiophen-3-yl-acrylic acid (**31**)

Piperidine (0.58 mL, 5.9 mmol) was added dropwise, at 0 °C, over a period of 10 min to a solution of thianaphten-3-carboxyaldehyde (**30**) (600 mg, 3.69 mmol) and malonic acid (1.9 g, 18.45 mmol), in pyridine (8 mL). The title compound **31** was obtained in 95% yield (750 mg, 3.50 mmol) as a white solid; ^{1}H NMR (400 MHz, DMSO-d_6) δ (ppm): 6.63 (d, J = 16 Hz, 1H), 7.47 (m, 2H), 7.88 (d, J = 16 Hz, 1H), 8.07 (d, J = 8.1 Hz, 1H), 8.08 (d, J = 8.26 Hz, 1H), 8.39 (s, 1H); ^{13}C NMR (100 MHz, DMSO-d_6) δ (ppm): 119.5, 121.8, 123.1, 124.9, 125.0, 129.4, 130.7, 135.2, 136.7, 139.7, 167.5.

4.8. 2H-benzo[4,5]thieno[2,3-c]pyridin-1-one (**14**)

Triethylamine (0.49 mL, 3.8 mmol) and ethylchloroformate (0.36 mL, 3.8 mmol) were sequentially added, at 0 °C, to a stirred solution of 3-benzo[b]thiophen-3-yl-acrylic acid (**31**) (600 mg, 2.92 mmol), in acetone (60 mL). Stirring was continued for 20 min at room temperature. Sodium azide (227.7 mg, 3.5 mmol) was then added at 0 °C to the mixture and the resulting suspension was reacted additionally 30 min at room temperature. The crude was filtrated under vacuo, the filtrate was carefully concentrated under reduced pressure to afford crude acyl azide intermediate (not shown) used then without further purification. A solution above azide in diphenyl ether (5 mL) was warmed at 230 °C for 30 min in presence of tri-buthylamine (5.8 mmol). The mixture was allowed to cool to room temperature, and the crude was purified by flash chromatography, eluting with CH$_2$Cl$_2$/MeOH as gradient from 0 to 5%. The title compound **14** was obtained in 45% yield as gray solid; mp 276 °C; ^{1}H NMR (400 MHz, DMSO-d_6) δ (ppm): 7.20 (d, J = 6.8 Hz, 1H), 7.48 (d, J = 6.8 Hz, 1H), 7.53 (dt, J_d = 1.9 Hz, J_t = 7.2 Hz, 1H), 7.61 (dt, J_d = 1.4 Hz, J_t = 7.2 Hz, 1H), 8.12 (d, J = 8.0 Hz, 1H), 8.3 (d, J = 8.5 Hz, 1H), 11.8 (s, 1H); ^{13}C NMR (100 MHz, DMSO-d_6) δ (ppm): 100.0, 123.4, 123.7, 124.9, 128.1, 128.3, 131.2, 134.8, 140.7, 142.0, 158.6; MS (ESI$^+$) m/z for C$_{11}$H$_8$NOS (M+H)$^+$ calcd: 202.0321, found: 202.0323.

4.9. 3-Phenyl[1]benzothieno[2,3-c]pyridin-1(2H)-one (**16**)

BuLi 2.5 M in hexane (2.08 mL) was added to a stirred solution of DIPA (0.15 mL, 1.04 mmol) in THF (5 mL) at −78 °C. Stirring was continued for additional 25 min, and then a solution of 3-methylbenzo[b]thiophene-2-carboxylic acid **32** (500 mg, 2.6 mmol) in THF (5 mL) was added dropwise to the reaction mixture. After the addition was complete stirring was continued at 0 °C for 1 h. The mixture was cooled to −78 °C and a solution of benzonitrile (**33**) (0.26 mL, 2.6 mmol) in THF (5 mL) was added slowly at the same temperature. Stirring was continued at room temperature for 24 h. The crude of reaction was diluted with water (20 mL) acidified to pH 3 and extracted with EtOAc (3 × 20 mL). The collected organic layers were filtered off. The collected white solid was anhydrified under reduced pressure. The filtrate was washed with brine dried over Na$_2$SO$_4$ and concentrated under vacuum. The title compound **16** was obtained in 49% yield (350 mg, 1.26 mmol), as white solid; mp > 280 °C; ^{1}H NMR (400 MHz, DMSO-d_6) δ (ppm): 7.40−7.54 (m, 3H), 7.56−7.63 (m, 3H), 7.87 (d, J = 8.2 Hz, 2H), 8.13 (d, J = 7.7 Hz, 1H), 8.45 (d, J = 7.5 Hz, 1H), 12.05 (s, 1H); ^{13}C NMR (100 MHz, DMSO-d_6) δ (ppm): 99.9, 123.5, 124.0, 124.9, 126.9 (2C), 127.0, 128.2, 128.6 (2C), 129.3, 133.5, 135.0, 141.0, 142.2, 142.9, 159.7; MS (ESI$^+$) m/z for C$_{17}$H$_{12}$NOS (M+H)$^+$ calcd: 278.0634, found: 278.06209.

4.10. 3-Amino-benzo[b]thiophene-2-carboxylic acid methyl ester (**36**)

A solution of KOH (3.5 M, 74.34 mmol) was added dropwise at 0 °C to a solution of 2-fluorobenzonitrile (**34**) (5 g, 41.3 mmol) and methylthioglycolate (**35**) (3.7 mL, 41.3 mmol) in DMF (70 mL). Stirring was continued at this temperature for additional 1 h. The mixture was poured in ice-water and extracted with EtOAc (3 × 50 mL). The organic phases were washed with brine, dried over Na$_2$SO$_4$, and concentrated in vacuo. The crude was purified by flash chromatography eluting with PET/EtOAc (from 2% to 20%) plus 5% of DCM to avoid product crystallization and affording the title compound **36** in 40% yield (3.30 g, mmol). ^{1}H NMR (200 MHz, CDCl$_3$) δ (ppm): 3.90 (s, 3H), 7.19−7.84 (m, 4H). Further analytical data are in agreement with those reported elsewhere [31].

4.11. Preparation of 3-carboxamido-benzo[b]thiophene-2-carboxylic acid methyl esters **37–41**

General procedure D: the corresponding carbonyl chloride (0.5 mL, 4.06 mmol) was added dropwise at 0 °C to a solution of **36** (700 mg, 3.38 mmol) and Et$_3$N (0.7 mL, 5.07 mmol) in DCM (14 mL). Stirring was continued at rt from 24 to 48 h. The mixture was poured in water (40 mL) and extracted with DCM (3 × 10 mL); the organic phases were washed with brine, dried over Na$_2$SO$_4$ and concentrated under reduced pressure. The crude was purified by flash chromatography eluting with PET/EtOAc (from 2% to 20%) plus 5% of DCM to avoid product crystallization.

4.11.1. 3-Benzoylamino-benzo[b]thiophene-2-carboxylic acid methyl ester (**37**)
Yield 31%; ^{1}H NMR (200 MHz, DMSO-d_6) δ (ppm): 3.83 (s, 3H), 7.20-8.10 (m, 9H), 10.52 (s, 1H).

4.11.2. 3-(Cyclohexanecarbonyl-amino)-benzo[b]thiophene-2-carboxylic acid methyl ester (38)

Yield quantitative; ^{1}H NMR (400 MHz, DMSO-d_6) δ (ppm): 1.19-1.36 (m, 4H), 1.40–1.47 (m, 2H), 1.78 (d, J = 12.6 Hz, 2H), 1.93 (d, J = 11.5, 2H), 3.81 (s, 1H), 2.47-2.50 (m, 1H), 7.46 (t, J = 7.3 Hz, 1H), 7.55 (t, J = 7.3 Hz, 1H), 7.75 (d, J = 8.0 Hz, 1H), 8.00 (d, J = 8.1 Hz, 1H), 9.98 (s, 1H).

4.11.3. 3-[(Thiophene-2-carbonyl)-amino]-benzo[b]thiophene-2-carboxylic acid methyl ester (39)

Yield 16%; ^{1}H NMR (400 MHz, CDCl₃) δ (ppm): 3.87 (s, 3H) 7.00 (dd, J_d = 3.8 Hz, J_d = 4.9 Hz, 1H), 7.44 (t, J = 8.1 Hz, 1H), 7.53 (t, J = 8.1 Hz, 1H), 7.55 (d, J = 3.8 Hz, 1H), 7.61 (d, J = 4.9 Hz, 1H), 7.81 (d, J = 8.1 Hz, 1H), 7.87 (d, J = 8.2 Hz, 1H).

4.11.4. 3-(4-Methyl-benzoylamino)-benzo[b]thiophene-2-carboxylic acid methyl ester (40)

Yield 40%; ^{1}H NMR (400 MHz, CDCl₃) δ (ppm): 2.47 (s, 3H), 3.96 (s, 3H), 7.36 (d, J = 7.8 Hz, 2H), 7.44 (t, J = 8.2 Hz, 1H), 7.52 (t, J = 8.1 Hz, 1H), 7.81 (d, J = 8.1 Hz, 1H), 8.00 (d, J = 8.18 Hz, 1H), 8.27 (d, J = 8.2 Hz, 1H), 10.53 (s, 1H).

4.11.5. 3-(4-tert-Butyl-benzoylamino)-benzo[b]thiophene-2-carboxylic acid methyl ester (41)

Yield 40%; ^{1}H NMR (200 MHz, CDCl₃) δ (ppm): 1.38 (s, 9H), 3.94 (s, 3H), 7.47 (t, J = 8.4 Hz, 2H), 7.57 (d, J = 8.4 Hz, 2H), 7.79 (d, J = 7.7 Hz, 1H), 8.04 (d, J = 8.4 Hz, 2H), 8.26 (d, J = 7.7 Hz, 1H), 10.57 (s, 1H).

4.12. Preparation of 2-substituted-3H-benzo[4,5]thieno[3,2-d]pyrimidin-4-ones 18, 20–23

General procedure E: A 30% ammonia solution (30 mL) was added to a suspension of the corresponding amide 37–41 (300 mg, 0.945 mmol) in MeOH (15 mL). Stirring was continued at reflux for 16 h. The mixture was cooled to rt, the volatile were removed under vacuo, the solid was collected, washed with water and hot methanol. Pure final compounds were obtained with variable yields.

4.12.1. 2-Phenyl-3H-benzo[4,5]thieno[3,2-d]pyrimidin-4-one (18)

Yield 39%; white solid, mp 327–328 °C; ^{1}H NMR (400 MHz, DMSO-d_6) δ (ppm): 7.55–7.61 (m, 3H), 7.66 (dd, J_d = 19.2 Hz, J_{dd} = 1.3 Hz, 1H), 7.68 (dd, J_d = 15.1 Hz, J_d = 1.3 Hz, 1H), 8.17 (d, J = 7.9 Hz, 1H), 8.26 (dd, J_d = 1.3 Hz, J_d = 7.8 Hz, 2H), 8.35 (d, J = 7.8 Hz, 1H), 13.00 (s, 1H). ^{13}C NMR (100.6 MHz, DMSO-d_6) δ (ppm): 121.0, 123.3, 123.8, 125.4, 127.8 (2C), 128.5 (2C), 129.1, 131.4, 132.1, 134.1, 140.3, 152.9, 154.8, 158.9; MS (ESI⁺) m/z for C₁₆H₁₁N₂OS (M+H)⁺ calcd: 279.0587, found: 279.0588.

4.12.2. 2-Cyclohexyl-3H-benzo[4,5]thieno[3,2-d]pyrimidin-4-one (20)

Yield 45%; white solid, mp 277–278; ^{1}H NMR (400 MHz, DMSO-d_6) δ (ppm): 1.28–1.35 (m, 3H), 1.67 (t, J = 11.1 Hz, 3H), 1.79 (d, J = 11.9 Hz, 2H), 1.93 (d, J = 12.0 Hz, 2H), 2.70–2.75 (m, 1H), 7.57 (t, J = 7.4 Hz, 1H), 7.64 (t, J = 7.4 Hz, 1H), 8.09 (d, J = 7.9, 1H), 8.22 (d, J = 7.7 Hz, 1H), 12.5 (s, 1H); ^{13}C NMR (100.6 MHz, DMSO-d_6) δ (ppm): 25.6, 25.8 (2C), 30.8 (2C), 43.0, 120.7, 123.8, 124.2, 125.8, 129.5, 134.5, 140.8, 153.6, 159.2, 164.0; MS (ESI⁺) m/z for C₁₆H₁₇N₂OS (M+H)⁺ calcd: 285.105, found 285.106.

4.12.3. 2-Thiophen-2-yl-3H-benzo[4,5]thieno[3,2-d]pyrimidin-4-one (21)

Yield 28%, yellowish solid, mp 338–340 °C; ^{1}H NMR (400 MHz, DMSO-d_6) δ (ppm): 7.25 (m, 1H), 7.62 (t, J = 7.8 Hz, 1H), 7.68 (t, J = 7.4 Hz, 1H), 7.87 (d, J = 4.9 Hz, 1H), 8.14 (d, J = 8.0 Hz, 1H), 8.24-8.26 (m, 2H), 13 (s, 1H). ^{13}C NMR (100.6 MHz, DMSO-d_6) δ (ppm): 121.0, 123.8, 124.4, 126.0, 129.1, 129.8, 130.1, 132.6, 134.2, 137.0, 140.9, 150.8, 153.3, 159.0; MS (ESI⁺) m/z for C₁₄H₉N₂OS₂ (M+H)⁺ calculated: 285.0151, found: 285.0152.

4.12.4. 2-p-Tolyl-3H-benzo[4,5]thieno[3,2-d]pyrimidin-4-one (22)

Yield 27%; white solid, mp 330–332 °C; ^{1}H NMR (400 MHz, DMSO-d_6) δ (ppm): 2.41 (s, 3H), 7.39 (d, J = 7.8 Hz, 2H), 7.62 (t, J = 7.5 Hz, 1H), 7.68 (t, J = 7.1 Hz, 1H), 8.15-8.19 (m, 3H), 8.36 (d, J = 7.9 Hz, 1H), 12.95 (s, 1H). ^{13}C NMR (100.6 MHz, DMSO-d_6) δ (ppm): 21.4, 29.4, 121.2, 123.9, 124.4, 125.9, 128.3 (2C), 129.7 (2C), 129.9, 134.7, 140.9, 142.1, 153.6, 155.4, 159.5; MS (ESI⁺) m/z for C₁₇H₁₃N₂OS (M+H)⁺ calcd: 293.0743, found: 293.0743.

4.12.5. 2-(4-tert-Butyl-phenyl)-3H-benzo[4,5]thieno[3,2-d]pyrimidin-4-one (23)

Yield 39%; white solid, mp: 329–331 °C; ^{1}H NMR (400 MHz, DMSO-d_6) δ (ppm): 1.34 (s, 9H), 7.59-7.64 (m, 3H), 7.69 (t, J = 8.0 Hz, 1H), 8.17-8.22 (m, 3H), 8.35 (d, J = 8.0 Hz, 1H), 13.00 (s, 1H); ^{13}C NMR (100.6 MHz, DMSO-d_6) δ (ppm): 31.3 (3C), 35.1, 121.3, 123.9, 124.4, 126.0 (3C), 128.2 (2C), 129.6, 129.9, 134.7, 140.9, 153.6, 154.9, 155.3, 159.5; MS (ESI⁺) m/z for C₂₀H₁₉N₂OS (M+H)⁺ calculated: 335.1213, found: 335.1218.

4.13. 2-Chloro-cyclohex-1-enecarbaldehyde (43)

Phosphorous oxychloride (1.5 mL, 16.3 mmol) was added at 0 °C (ice bath) to DMF (1.6 mL, 20.38 mmol). Stirring was continued at this temperature for 8 min after which the ice bath was replaced with a water bath and the mixture was stirred for additional 8 min. Cyclohexanone (42) (1.0 g, 10.19 mmol) was added at 0 °C to the above mixture, and stirring was continued at this temperature 15 min and at room temperature for additional 15 min. The crude was poured in ice and the pH was adjusted to 8 by the addition of NaHCO₃ (ss). The mixture was extracted with Et₂O (4 × 30 mL), the organic phases were collected, washed with NaHCO₃ (ss) and brine, and dried over Na₂SO₄. Evaporation of the volatile afforded the title compound 43 in 90% yield (1.32 g, 9.13 mmol) as a red oil.

^{1}H NMR (200 MHz, CDCl₃) δ (ppm): 1.67–1.77 (m, 4H), 2.30–2.32 (m, 2H), 2.58-2.61 (m, 2H), 10.19 (s,1H). Further analytical data are in agreement with those reported elsewhere [32].

4.14. 2-Chloro-cyclohex-1-enecarbonitrile (44)

Hydroxyl amine hydrochloride (761 mg, 10.9 mmol) was added to a solution of intermediate 43 (1.32 g, 9.13 mmol) in N-methyl-2-pyrrolidinone (15 mL). The mixture was stirred at 115 °C for 8 h. The crude was poured in water (50 mL) and extracted with EtOAc (4 × 10 mL). The organic phases were collected, washed with brine, dried over Na₂SO₄ and concentrated under reduced pressure. The crude material was purified by flash chromatography, eluting with PET/Et₂O (from 2% to 15%) affording the oxime intermediate (not shown) readily dehydrated upon treatment with refluxing acetic anhydride for 20 h. Aqueous work up of the mixture and flash chromatography purification of the reaction crude eluting with PET/Et₂O (from 2% to 15%) afforded the title compound 44 in 50% yield (646 mg, 4.56 mmol) as a colorless oil.

^{1}H NMR (400 MHz, CDCl₃) δ (ppm): 1.67–1.73 (m, 2H), 1.76–1.82 (m, 2H), 2.34–2.38 (m, 2H), 2.46-2.50 (m, 2H).

4.15. 3-Amino-4,5,6,7-tetrahydro-benzo[b]thiophene-2-carboxylic acid methyl ester (45)

Methylthioglycolate (0.2 mL, 2.74 mmol) and K₂CO₃ (378 mg, 2.74 mmol) were added in turn to a solution of 44 (388 mg, 2.74 mmol) in methanol (5 mL) and THF (1 mL). The mixture was

reacted at reflux for 16 h. The solvent was removed under reduced pressure. The crude was taken up with water (30 mL) and extracted with EtOAc (3 × 20 mL). The organic phases were collected, washed with brine and dried over Na_2SO_4. Evaporation of the solvent furnished the title compound **45** in 90% yield (521 mg, 2.47 mmol) as white solid. ^{1}H NMR (400 MHz, CDCl$_3$) δ (ppm): 1.83−1.85 (m, 4H), 2.33 (m, 2H), 2.69 (m, 2H), 3.82 (s, 3H). Further analytical data are in agreement with those reported elsewhere [36].

4.16. 3-Benzoylamino-4,5,6,7-tetrahydro-benzo[b]thiophene-2-carboxylic acid methyl ester (**46**)

Et$_3$N (0.3 mL, 1.91 mmol) and benzoyl chloride (0.2 mL, 1.53 mmol) were added in turn to a solution of **45** (269 mg, 1.27 mmol) in DCM (6 mL). Stirring was continued under inert atmosphere 48 h. The mixture was poured in water (30 mL) and extracted with DCM (3 × 20 mL). The organic phases were collected, washed with brine and dried over Na_2SO_4. The crude material was purified by flash chromatography eluting with PET/Et$_2$O (from 2% to 15%) affording the title compound **46** in 78% yield (312 mg, 0.98 mmol). ^{1}H NMR (200 MHz, CDCl$_3$) δ (ppm): 1.72−1.83 (m, 2H), 1.88-2.08 (m, 2H), 2.69 (t, J = 5.9 Hz, 2H), 2.85 (t, J = 5.9 Hz, 2H), 3.87 (s, 3H), 7.48−7.61 (m, 3H), 8.03 (d, J = 6.7 Hz, 2H), 10.00 (s, 1H).

4.17. 2-Phenyl-6,7,8,9-tetrahydro-3H-benzo[4,5]thieno[3,2-d]pyrimidin-4-one (**19**)

Following the general procedure E the title compound **19** has been obtained in 40% yield as white solid; mp 328−330 °C; ^{1}H NMR (400 MHz, DMSO-d_6) δ (ppm): 1.83-1.87 (m, 4H), 2.74 (m, 2H), 2.86 (m, 2H), 7.52−7.58 (m, 3H), 8.13 (d, J = 6.9 Hz, 2H), 12.58 (s, 1H). ^{13}C NMR (100.6 MHz, DMSO-d_6) δ (ppm): 21.81, 23.29, 23.35, 25.99, 118.80, 128.20 (2C), 129.06 (2C), 131.69, 132.29, 133.06, 145.91, 154.48, 156.93, 158.66; MS (ESI$^+$) m/z for $C_{16}H_{15}N_2OS$ (M+H)$^+$ calcd: 283.0900, found: 283.0901.

4.18. Molecular modeling

All the programs used are available in the Schrodinger Suite 2012 (Schrödinger Release 2012, LLC, New York, NY, 2012). The protein structures used in this study were submitted to the "*Protein Preparation Wizard*" protocol using the default settings to add hydrogens and check the structures. All the TNKS-1 and TNKS-2 PDBs up to when this study started (May 2012) were selected, choosing only the co-crystals with binders at the canonical site. A final list of eight co-crystals was obtained, belonging to four papers, with PDB codes: 3KR8 [23], 3MHJ/3MHK/3P0N/3P0P/3P0Q [8], 3U9H [14], and 3UH4 [22]. Applying a workflow similar to the one already used by our group in a previous VS as reported elsewhere [37], by the aim of the Phase program v. 3.4 [38] a pharmacophore hypothesis was generated through the "*manual creation*" procedure. The SPECS database (www.specs.net) was prepared for the calculations generating all the tautomers, isomers and ionization states through the *Ligprep* procedure of the Schrodinger Suite. A better computational time performance was achieved transforming the resulting data set in a *3D Phase* database through a standard procedure that adds a set of conformers to each molecule. Among the eight superimposed proteins, the excluded volumes were added selecting the side chain of each residue defining the protein binding site. In order to have a volume in the binding site as larger as possible, all the compact side chains were chosen, thus creating a less restrictive pharmacophore. The grid generation was done on the TNKS-2/XAV-939 crystal complex and all the docking runs were performed using Glide v 5.5 in extra-precision (*XP*) mode and leaving all the variables at default values. These settings were able to correctly

reproduce the observed crystallographic pose of the XAV939 compound. The Tanimoto clustering was performed using the CACTVS toolkit [39] and the SUBSET [40] routine. Marvin was used for the calculation of the logD values (Marvin 5.7.0, 2011, ChemAxon, http://www.chemaxon.com). All the images were taken by Maestro (Schrödinger Release 2012, LLC, New York, NY, 2012) and PYMOL programs [41].

4.19. Pharmacology

4.19.1. PARP assays

In general, all PARP assays were done by following the BPS PARP assay kit protocols (BPS Bioscience Inc, San Diego, USA) using human recombinant proteins (further data on SI). In particular, the enzymatic reactions for PARPs were conducted in duplicate at rt for 1 h in a 96 well plate coated with histone substrate. For TNKSs assay, GST-TNKSs was coated on the glutathione plate for the autoribosylation reaction, instead of histone. 50 μl of reaction buffer (Tris·HCl, pH 8.0) contains NAD+, biotinylated NAD+, activated DNA, a PARP enzyme and the test compound. For other PARP assays 50 μl of reaction buffer (Tris·HCl, pH 8.0) contains NAD+, biotinylated NAD+, activated DNA, a PARP enzyme and the test compound. After enzymatic reactions (1 h at RT for PARPs; 1 h at 30 °C for TNKSs), 50 μl of Streptavidin-horseradish peroxidase was added to each well and the plate was incubated at rt for an additional 30 min. 100 μl of developer reagents were added to wells and luminescence was measured using a BioTek Synergy™ 2 microplate reader. The luminescence data were analyzed using the computer software, Graphpad Prism. In the absence of the compound, the luminescence (Lt) in each data set was defined as 100% activity. In the absence of the PARP, the luminescence (Lb) in each data set was defined as 0% activity. The percent activity in the presence of each compound was calculated according to the following equation: % activity = [(L − Lb)/(Lt − Lb)] × 100, where L = the luminescence in the presence of the compound, Lb = the luminescence in the absence of the PARP, and Lt = the luminescence in the absence of the compound. The percent inhibition was calculated according to the following equation: % inhibition = 100 − % activity.

4.19.2. Wnt assay

To determine TCF-luciferase reporter activity, DLD-1 colorectal cancer cells were transduced with TOP-TCF reporter lentivirus expressing firefly luciferase together with renilla luciferase lentivirus (at a 1:20 ratio). The latter was used to normalize for infection efficiency. Compounds were tested at 10 μM concentration. DMSO was used as negative and compound **1** as positive controls, respectively. Twenty-four h after infection, cells were lysed and analyzed utilizing the dual luciferase reporter assay system (Promega, USA). Luciferase reporter activity was calculated by measuring the TOP/RL ratio. For colony growth assay, 5×10^3 DLD-1 cells were treated daily with 1 μM, 5 μM and 10 μM concentrations of compounds **1**, IWR-1 (**25**), and **23** dissolved in dimethyl sulfoxide, or the latter alone (negative control). After 10 days, cells were fixed in 10% methanol/acetic acid solution and stained with 1% crystal violet (in methanol) for quantification. Image J program was used for the quantification analysis. We examined the dose−response curves for XAV939 (**1**), IWR1 (**25**), and **23**. We found that they are not well represented by a monotonic sigmoid function. We took a standard approach to IC$_{50}$ estimation by modeling the dose response curve with the following monotonic sigmoidal function:

$$\text{Response} = \frac{a - d}{1 - \left(\frac{\text{Dose}}{c}\right)^b} + d$$

Where a, b, c, d are parameters. We estimate the parameters by numerically minimizing the residuals (the difference between the data and the model) across all three experimental replicates. Calculations were performed on the Mathematical platform. We used the best fit model to estimate the IC_{50} values by inversion of the model function. In addition, we were able to use the experimental replicates and derive models for the upper and lower 95% confidence bands using the same numerical minimization method.

Notes

All co-authors have agreed with the submission of the final manuscript and participated in the research.

Acknowledgments

Appendix A. Supplementary data

Supplementary data related to this article can be found at http://dx.doi.org/10.1016/j.ejmech.2014.10.007.

References

[1] A. Hakmé, H.K. Wong, F. Dantzer, V. Schreiber, The expanding field of poly(ADP-ribosyl)ation reactions. 'Protein modifications: beyond the usual suspects' review series, EMBO Rep. 9 (2008) 1094—1100.

[2] M.O. Hottinger, P.O. Hassa, B. Luscher, H. Schüler, F. Koch-Nolte, Toward a unified nomenclature for mammalian ADP-ribosyltransferases, Trends Biochem. Sci. 35 (2010) 208—219.

[3] J.L. Riffell, C.J. Lord, A. Ashworth, Tankyrase-targeted therapeutics: expanding opportunities in the PARP family, Nat. Rev. Drug. Discov. 11 (2012) 923—936.

[4] Z. Li, Y. Yamauchi, M. Kamakura, T. Murayama, F. Goshima, H. Kimura, Y. Nishiyama, Herpes simplex virus requires poly(ADP-ribose) polymerase activity for efficient replication and induces extracellular signal-related kinase-dependent phosphorylation and ICP0-dependent nuclear localization of tankyrase 1, J. Virol. 86 (2012) 492—503.

[5] Z. Deng, C. Atanasiu, K. Zhao, R. Marmorstein, J.I. Sbodio, N.-W. Chi, P.M. Lieberman, Inhibition of Epstein-Barr virus OriP function by tankyrase, a telomere-associated poly-ADP ribose polymerase that binds and modifies EBNA1, J. Virol. 79 (2005) 4640—4650.

[6] A. Ulsamer, Y. Wei, K.K. Kim, K. Tan, S. Wheeler, Y. Xi, R.S. Thies, H.A. Chapman, Axin pathway activity regulates in vivo pY654-beta-catenin accumulation and pulmonary fibrosis, J. Biol. Chem. 287 (2012) 5164—5172.

[7] T.Y.J. Yeh, K.K. Beiswenger, P. Li, K.E. Bolin, R.M. Lee, T.S. Tsao, A.N. Murphy, A.L. Hevener, N.W. Chi, Hypermetabolism, hyperphagia, and reduced adiposity in tankyrase-deficient mice, Diabetes 58 (2009) 2476—2485.

[8] E. Wahlberg, T. Karlberg, E. Kouznetsova, N. Markova, A. Macchiarulo, A.G. Thorsell, E. Pol, A. Frostell, T. Ekblad, D. Oncü, B. Kull, G.M. Robertson, R. Pellicciari, H. Schüler, J. Weigelt, Family-wide chemical profiling and structural analysis of PARP and tankyrase inhibitors, Nat. Biotechnol. 30 (2012) 283—288.

[9] S.M. Huang, Y.M. Mishina, S. Liu, A. Cheung, F. Stegmeier, G.A. Michaud, O. Charlat, E. Wiellette, Y. Zhang, S. Wiessner, M. Hild, X. Shi, C.J. Wilson, C. Mickanin, V. Myer, A. Fazal, R. Tomlinson, F. Serluca, W. Shao, H. Cheng, M. Shultz, C. Rau, M. Schirle, J. Schlegl, S. Ghidelli, S. Fawell, C. Lu, D. Curtis, M.W. Kirschner, C. Lengauer, P.M. Finan, J.A. Tallarico, T. Bouwmeester, J.A. Porter, A. Bauer, F. Cong, Tankyrase inhibition stabilizes axin and antagonizes Wnt signalling, Nature 461 (2009) 614—620.

[10] E.A. Larsson, A. Jansson, F.M. Ng, S.W. Then, R. Panicker, B. Liu, K. Sangthongpitag, V. Pendharkar, S.J. Tai, J. Hill, C. Dan, S.Y. Ho, W.W. Cheong, A. Poulsen, S. Blanchard, G.R. Lin, J. Alam, T.H. Keller, P. Nordlund, Fragment-based ligand design of novel potent inhibitors of tankyrases, J. Med. Chem. 56 (2013) 4497—4508.

[11] T. Haikarainen, J. Koivunen, M. Narwal, H. Venkannagari, E. Obaji, P. Joensuu, T. Pihlajaniemi, L. Lehtiö, para-Substituted 2-phenyl-3,4-dihydroquinazolin-4-ones as potent and selective tankyrase inhibitors, ChemMedChem 8 (2013) 1978—1985.

[12] M.D. Shultz, D. Majumdar, D. Chin, P.D. Fortin, Y. Feng, T. Gould, C.A. Kirby, T. Stams, N.J. Waters, W. Shao, Structure—efficiency relationship of [1,2,4]triazol-3-ylamines as novel nicotinamide isosteres that inhibit tankyrases, J. Med. Chem. 56 (2013) 7049—7059.

[13] P. Liscio, A. Carotti, S. Asciutti, T. Karlberg, D. Bellocchi, L. Llacuna, A. Macchiarulo, S.A. Aaronson, H. Schüler, R. Pellicciari, E. Camaioni, Design, synthesis, crystallographic studies, and preliminary biological appraisal of

[14] new substituted triazolo[4,3-b]pyridazin-8-amine derivatives as tankyrase inhibitors, J. Med. Chem. 57 (2014) 2807—2812.

[14] B. Chen, M.E. Dodge, W. Tang, J. Lu, Z. Ma, C.W. Fan, S. Wei, W. Hao, J. Kilgore, N.S. Williams, M.G. Roth, J.F. Amatruda, C. Chen, L. Lum, Small molecule-mediated disruption of Wnt-dependent signaling in tissue regeneration and cancer, Nat. Chem. Biol. 5 (2009) 100—107.

[15] M. Narwal, H. Venkannagari, L. Lehtiö, Structural basis of selective inhibition of human tankyrases, J. Med. Chem. 55 (2012) 1360—1367.

[16] H. Gunaydin, Y. Gu, X. Huang, Novel binding mode of a potent and selective tankyrase inhibitor, PLoS One 7 (2012) e33740.

[17] J. Waaler, O. Machon, J.P. von Kries, S.R. Wilson, E. Lundenes, D. Wedlich, D. Gradl, J.E. Paulsen, O. Machonova, J.L. Dembinski, H. Dinh, S. Krauss, Novel synthetic antagonists of canonical Wnt signaling inhibit colorectal cancer cell growth, Cancer Res. 71 (2011) 197—205.

[18] A. Voronkov, D.D. Holsworth, J. Waaler, S.R. Wilson, B. Ekblad, H. Perdreau-Dahl, H. Dinh, G. Drewes, C. Hopf, J.P. Morth, S. Krauss, Structural basis and SAR for G007-LK, a lead stage 1,2,4-triazole based specific tankyrase 1/2 inhibitor, J. Med. Chem. 56 (2013) 3012—3023.

[19] H. Bregman, N. Chakka, A. Guzman-Perez, H. Gunaydin, Y. Gu, X. Huang, V. Berry, J. Liu, Y. Teffera, L. Huang, B. Egge, E.L. Mullady, S. Schneider, P.S. Andrews, A. Mishra, J. Newcomb, R. Serafino, C.A. Strathdee, S.M. Turci, C. Wilson, E.F. Dimauro, Discovery of novel, induced-pocket binding oxazolidinones as potent, selective, and orally bioavailable tankyrase inhibitors, J. Med. Chem. 56 (2013) 4320—4342.

[20] Z. Hua, H. Bregman, J.L. Buchanan, N. Chakka, A. Guzman-Perez, H. Gunaydin, X. Huang, Y. Gu, V. Berry, J. Liu, Y. Teffera, L. Huang, B. Egge, R. Emkey, E.L. Mullady, S. Schneider, P.S. Andrews, L. Acquaviva, J. Dovey, A. Mishra, J. Newcomb, D. Saffran, R. Serafino, C.A. Strathdee, S.M. Turci, M. Stanton, C. Wilson, E.F. Dimauro, Development of novel dual binders as potent, selective, and orally bioavailable tankyrase inhibitors, J. Med. Chem. 56 (2013) 10003—10015.

[21] P. Liscio, E. Camaioni, A. Carotti, R. Pellicciari, A. Macchiarulo, From polypharmacology to target specificity: the case of PARP inhibitors, Curr. Top. Med. Chem. 13 (2013) 2939—2954.

[22] C.A. Kirby, A. Cheung, A. Fazal, M.D. Shultz, T. Stams, Structure of human tankyrase 1 in complex with small-molecule inhibitors PJ34 and XAV939, Acta Crystallogr. Sect. F. 68 (2012) 115—118.

[23] T. Karlberg, N. Markova, I. Johansson, M. Hammarström, P. Schütz, J. Weigelt, H. Schüler, Structural basis for the interaction between tankyrase-2 and a potent Wnt-signaling inhibitor, J. Med. Chem. 53 (2010) 5352—5355.

[24] S. Pakray, N.R. Castle, The synthesis of dimethoxy[l]benzothieno[2,3-c]quinolines, J. Het. Chem. 23 (1986) 1571—1577.

[25] J.D. McKenney, N.R. Castle, The synthesis of [l]benzothieno[2,3-c]quinolines, [l]benzothieno[2,3-c][1,2,4]triazolo[4,3-a]quinoline, and [l]benzothieno[2,3-c]tetrazolo[1,5-a]quinoline, J. Het. Chem. 24 (1987) 1525—1529.

[26] S.L. Castle, P.J. Buckhaults, L.J. Baldwin, J.D. McKenney, N.R. Castle, The synthesis of monomethoxy[l]benzothieno[2,3-c]quinolines, J. Het. Chem. 24 (1987) 1103—1108.

[27] K. Gorlitzer, B. Gabriel, P. Frohberg, G. Drutkowski, J. Wiesner, H. Jomaa, Thieno[2,3-c]chinoline — synthese und biologische prüfung, Pharmazie 59 (2004) 439—442.

[28] S. Chorbadjiev, Synthesis of 2-hydroxyquinolines from 2-amino-benzophenones and N,N-dimethylacetamide, Synth. Commun. 20 (1990) 3497—3505.

[29] V.O. Iaroshenko, S. Ali, T.M. Babar, M.S.A. Abbasi, V.Y. Sosnovskikh, A. Villinger, A. Tolmachev, P. Langer, Efficient synthesis of novel thieno[3,2-b]-, [2,3-c]- and [3,2-c]pyridones by Sonogashira coupling of bromothiophenes with terminal alkynes and subsequent intramolecular C-N bond-forming reaction, Tetrahedron 69 (2013) 3167—3181.

[30] I. Abdillahi, G. Kirsch, Synthesis of a novel series of thieno[3,2-d]pyrimidin-4-(3H)-ones, Synthesis 9 (2010) 1428—1430.

[31] R.J. Beck, J.A. Yahner, Synthesis of [l]benzothieno[3,2-d]pyrimidine derivatives, J. Org. Chem. 38 (1973) 2450—2452.

[32] G. Kuchenbeiser, A.R. Shaffer, N.C. Zingales, J.F. Beck, J.A.R. Schmidt, Palladium(II) 3-iminophosphine (3IP) complexes: active precatalysts for the intermolecular hydroamination of 1,2-dienes (allenes) and 1,3-dienes with aliphatic amines under mild conditions, J. Organomet. Chem. 696 (2011) 179—187.

[33] K.A. Menear, C. Adcock, R. Boulter, X.L. Cockcroft, L. Copsey, A. Cranston, K.J. Dillon, J. Drzewiecki, S. Garman, S. Gomez, H. Javaid, F. Kerrigan, C. Knights, A. Lau, V.M. Loh, I.T. Matthews, S. Moore, M.J. O'Connor, G.C. Smith, N.M. Martin, 4-[3-(4-cyclopropanecarbonylpiperazine-1-carbonyl)-4-fluorobenzyl]-2H-phthalazin-1-one: a novel bioavailable inhibitor of poly(ADP-ribose) polymerase-1, J. Med. Chem. 51 (2008) 6581—6591.

[34] T. Haikarainen, M. Narwal, P. Joensuu, L. Lehtiö, Evaluation and structural basis for the inhibition of tankyrases by PARP inhibitors, ACS Med. Chem. Lett. 20 (2013) 18—22.

[35] M. Aleksić, B. Bertoša, R. Nhili, L. Uzelac, I. Jarak, S. Depauw, M.H. David-Cordonnier, M. Kralj, S. Tomić, G. Karminski-Zamola, Novel substituted benzothiophene and thienothiophene carboxanilides and quinolones: synthesis, photochemical synthesis, DNA-binding properties, antitumor evaluation and 3D-derived QSAR analysis, J. Med. Chem. 55 (2012) 5044—5060.

[36] L. Tenora, M. Buchlovič, S. Man, M. Potáček, A new facile synthesis of methyl 3-amino-4,5,6,7-tetrahydrobenzo[b]thiophene-2-carboxylate, Tetrahedron Lett. 52 (2011) 401—403.

[37] M. Marinozzi, A. Carotti, E. Sansone, A. Macchiarulo, E. Rosatelli, R. Sardella, B. Natalini, G. Rizzo, L. Adorini, D. Passeri, F. De Franco, M. Pruzanski, R. Pellicciari, Pyrazole[3,4-e][1,4]thiazepin-7-one derivatives as a novel class of farnesoid X receptor (FXR) agonists, Bioorg. Med. Chem. 20 (2012) 3429–3445.

[38] S.L. Dixon, A.M. Smondyrev, S.N. Rao, PHASE: a novel approach to pharmacophore modeling and 3D database searching, Chem. Biol. Drug Des. 67 (2006) 370–372.

[39] W.D. Ihlenfeldt, Y. Takahashi, H. Abe, S. Sasaki, Computation and management of chemical properties in CACTVS: an extensible networked approach toward modularity and compatibility, J. Chem. Inf. Comput. Sci. 34 (1994) 109.

[40] J.H. Voigt, B. Bienfait, S. Wang, M.C. Nicklaus, Comparison of the NCI open database with seven large chemical structural databases, J. Chem. Inf. Comput. Sci. 41 (2001) 702–712.

[41] L.L. DeLano, The PyMOL Molecular Graphics System, 2002. http://www.pymol.org/.